Formation of xenon line profiles

E.P. Skorokhod, M.E. Kuli-zade, A.Yu. Gavrilova, and A.G. Kiselev

Moscow State Aviation Institute (University of Aerospace Technology)

Received October 7, 2001

The characteristics of xenon line profiles in absorption spectra of inhomogeneous low-temperature plasma are investigated within the framework of the collision-radiant meta-equilibrium model. Broadening constants for xenon line profiles are calculated. The broadening mechanisms for xenon spectral lines are considered. Tabular data allowing determination of the electron concentrations from xenon line widths in the case of two-temperature meta-equilibrium plasma are presented.

Introduction

Analysis of spectral line profiles of inert gas plasma is rather efficient in diagnostics for determination of parameters of the plasma under study. The problems of determination of plasma parameters from radiation characteristics are formally classified as inverse and ill-posed problems. The use of the calculated widths of xenon line profiles for diagnostic purposes[1] not always gives the desired result. The main difficulties are connected with two important problems, namely, variation of parameters of the plasma itself along the observation beam and the absence of theoretical recommendations in diagnostics of the thermally nonequilibrium two-temperature plasma.

The two-temperature quasi-stationary plasma possesses some features[2,3] distinguishing it from the thermally equilibrium plasma considered in the LTE model. The dependences described by the Saha–Boltzmann equations are violated. They are replaced with diagrams of meta-equilibrium states[2,3] being the results of solution of sublevel stationary kinetics. Such plasma is characterized by variation of the electron temperature $T_e \approx (0.8 \pm 0.2)$ eV for the wide range of variation of the electron concentration N_e and the density of particles (number of nuclei).

In Ref. 2, we considered in detail the distribution of excited states of the two-temperature meta-equilibrium plasma[3] of inert gases. In this paper, the emphasis is on the photon distributions or line profiles in the case of meta-equilibrium xenon plasma.

Broadening of spectral lines of xenon atom

To estimate the line widths of the two-temperature meta-equilibrium plasma, classic concepts are useful.[4] According to the collision theory, the main role in the broadening is played by particle transits within the Weiskopf radius

$$\rho_n = (\alpha_n C_n / v)^{1/(n-1)}. \quad (1)$$

Variation of the phase for the time of one collision can be written as

$$\eta = \int_{-\infty}^{\infty} \frac{C_n \mathrm{d}t}{(\rho^2 + v^2 t^2)^{n/2}}. \quad (2)$$

Here C_n are the interaction constants; v is the mean speed of a flying particle; $\alpha_n = \sqrt{\pi}\,\Gamma(n - 1/2) \times \times \Gamma(n/2)$; and the collision width is

$$\gamma_n = 2\pi N_e v \rho_n. \quad (3)$$

The line broadening is affected by various interactions with charged and neutral particles, namely, the square Stark effect ($n = 4$), linear Stark effect ($n = 2$), van der Waals ($n = 6$), and resonance ($n = 3$) broadening.

For convenience, let us introduce the following designations, as in Ref. 5:

$$\bar{C}_3 = C_3 \cdot 10^8 \ (\mathrm{cm}^3/\mathrm{s}),\ \bar{C}_4 = C_4 \cdot 10^{14} \ (\mathrm{cm}^4/\mathrm{s}),$$

$$\bar{C}_6 = C_6 \cdot 10^{32} \ (\mathrm{cm}^6/\mathrm{s}). \quad (4)$$

The power parameters (T, $\hbar\omega$, γ, Δ, etc.) are expressed in electronvolts, and the concentrations are expressed in 10^{18} cm^{-3} ($N_{e,a} = 10^{18} \cdot n_{e,a}$).

By the Weiskopf–Lindholm theory, the line width for the square Stark broadening can be presented as

$$\gamma_4 = 11.4 C_4^{2/3} v^{1/3} N_e; \quad (5)$$

$$\Delta_4 = 9.8 C_4^{2/3} v^{1/3} N_e. \quad (6)$$

The constant of square Stark broadening includes all transitions from a given level to upper and lower ones. Every transition was taken into account with its statistical weight g:

$$C_4 = \frac{e^4\hbar}{4\pi m} \sum \frac{f}{(\hbar\omega)^2},\ C_{4(nl)} = \frac{1.18}{g_{nl}} \sum_{n'l'} \frac{g f(nl \to n'l')}{(\hbar\omega)^2_{nl,n'l'}}. \quad (7)$$

The final equations for the line width determined by the electron $\gamma_{4,e}$ and ion $\gamma_{4,i}$ impact take the form:

$$\gamma_{4,e} = 1.41 \cdot 10^{-3} n_e (\bar{C}_4)^{2/3} (T_e)^{1/6},$$

$$\gamma_{4,i} = 1.78 \cdot 10^{-4} n_i (\bar{C}_4)^{2/3} (T_i)^{1/6}. \quad (8)$$

The broadening of the line profile by neutral particles is taken into account in the van der Waals

0235-6880/01/11 964-05 $02.00

mechanism. The interaction constant C_6 is calculated most often by the approximate equation[4]:

$$C_6 = e^2\alpha\bar{R}^2/\hbar. \quad (9)$$

In Eq. (9), α is the polarizability of the perturbed atom; $\bar{R}^2$ is the mean squared radius of the orbit corresponding to the excited state of the emitting atom

$$\bar{R}^2 = a_0^2 n^{*2}\{5n^{*2} + 1 - 3l(l + 1)\}/(2Z), \quad (10)$$

where n^* is the effective quantum number; l is the orbital moment. After transformation (7) we have

$$\bar{C}_6 = 0.391\frac{n^{*2}}{2Z}\{5n^{*2} + 1 - 3l(l + 1)\}. \quad (11)$$

The line width in this case is

$$\gamma_6 = 1.02\cdot10^{-6}(\bar{C}_6)^{2/5}(T_a)^{3/10}n_a \quad (12)$$

and the shift is

$$\Delta_6 = 2.96C_6^{2/5}v^{3/5}N_a. \quad (13)$$

The resonance broadening is practically significant only for the transitions involving the ground state.[5] The line width γ_3 is connected with the oscillator strength f_{abs} by the equation

$$\gamma_3 = 4\,\frac{e^2}{m}\frac{f_{abs}}{\hbar\omega}\,N_a\sqrt{\frac{2J_0 + 1}{2J_1 + 1}}, \quad (14)$$

where N_a is the concentration of atoms; J_0 and J_1 are the total moments of the atom in the ground ($5p^6\,{}^1S_0$) and excited ($5p^5ns$, $5p^5nd$) states involved in the main dipole transition ($J_1 = 1$). According to Eqs. (1) and (2), we have

$$\gamma_3 = 2\pi\alpha_3C_3N_a, \quad (15)$$

where

$$C_3 = 3.05\cdot10^{-8}f_{abs}/\hbar\omega. \quad (16)$$

Then the equations for calculation of the line width γ_3 take the form

$$\gamma_3 = 8.33\cdot10^{-5}n_a\bar{C}_3. \quad (17)$$

It should be noted that the resonance broadening, unlike other mechanisms, is independent of temperature.

Table 1 gives the calculated energy levels and constants $\bar{C}_3$, $\bar{C}_4$, and $\bar{C}_6$ (Ref. 6).

The line width is determined as

$$\gamma = \gamma_{4e} + \gamma_{\langle\sigma v\rangle} + \gamma_3 + \gamma_6, \quad (18)$$

where $\gamma_{\langle\sigma v\rangle}$ is the width caused by inelastic collisions with electrons.[5]

The experimentally measured xenon line widths obtained from the spectra reported in Ref. 10 and those calculated theoretically by Eq. (18) are given in Table 2. It should be noted that some values for the *s*-*p*-transitions coincide or differ approximately two times. For the *d*-states, the most probable decay channel of the molecular ion, the widths of the *p*-*d*-transitions differ ten times.

Table 1. Values of the main quantum numbers, energy levels, and broadening constants $\bar{C}_3$, $\bar{C}_4$, and $\bar{C}_6$

#	Level	n^*	E, eV	$\bar{C}_3$	$\bar{C}_4$	$\bar{C}_6$
1	$6s[3/2]_1$	1.919296	8.436	14	0.75	14
2	$7s[3/2]_1$	2.975527	10.592	78	12.1	78
3	$8s[3/2]_1$	3.987458	11.274	250	60	250
4	$6s[3/2]_2$	1.888554	8.315	–	0.6	13
5	$7s[3/2]_2$	2.945823	10.561	–	8.4	75
6	$8s[3/2]_2$	3.951016	11.257	–	21	240
7	$6p[1/2]_0$	2.488849	9.932	–	−15	32
8	$7p[1/2]_0$	3.493408	11.014	–	−27	130
9	$8p[1/2]_0$	4.559365	11.475	–	–	400
10	$6p[1/2]_1$	2.309966	9.579	–	1.8	23
11	$7p[1/2]_1$	3.328154	10.901	–	44	110
12	$8p[1/2]_1$	4.395120	11.425	–	–	350
13	$6p[3/2]_1$	2.410965	9.789	–	2.6	27
14	$7p[3/2]_1$	3.474583	11.002	–	60	130
15	$8p[3/2]_1$	4.466373	11.447	–	–	370
16	$6p[3/2]_2$	2.427514	9.82	–	3.7	28
17	$7p[3/2]_2$	3.463531	10.995	–	470	130
18	$8p[3/2]_2$	4.481798	11.452	–	–	375
19	$6p[5/2]_2$	2.359279	9.685	–	2	25
20	$7p[5/2]_2$	3.401835	10.953	–	53	120
21	$8p[5/2]_2$	4.421704	11.433	–	–	355
22	$6p[5/2]_3$	2.376416	9.72	–	2.3	26
23	$7p[5/2]_3$	3.423111	11.005	–	80	120
24	$8p[5/2]_3$	4.43898	11.432	–	–	360
25	$5d[1/2]_0$	2.464777	9.89	16	1.3	16
26	$6d[1/2]_0$	3.427102	10.97	96	−15	96
27	$7d[1/2]_0$	4.436948	11.438	310	−280	310
28	$5d[1/2]_1$	2.47967	9.917	17	4.8	17
29	$6d[1/2]_1$	3.437937	10.978	97	36	97
30	$7d[1/2]_1$	4.385481	11.42	300	1400	300
31	$5d[3/2]_1$	2.805277	10.4	34	0.94	34
32	$6d[3/2]_1$	3.750338	11.162	150	24	150
33	$7d[3/2]_1$	4.629578	11.495	375	−110	375
34	$5d[3/2]_2$	2.496709	9.958	17	−1.8	17
35	$6d[3/2]_2$	3.467703	10.998	100	−450	100
36	$7d[3/2]_2$	4.632927	11.495	380	−5	380
37	$5d[5/2]_2$	2.626362	10.157	24	−0.8	24
38	$6d[5/2]_2$	3.574013	11.064	120	−12	120
39	$7d[5/2]_2$	4.613565	11.49	370	−40	370
40	$5d[5/2]_3$	2.669041	10.219	26	−0.7	26
41	$6d[5/2]_3$	3.636195	11.112	130	0.1	130
42	$7d[5/2]_3$	4.638419	11.5	380	−30	380
43	$5d[7/2]_3$	2.550903	10.039	20	−0.9	20
44	$6d[7/2]_3$	3.52943	11.037	110	−14	110
45	$7d[7/2]_3$	4.599136	11.486	370	−33	370
46	$5d[7/2]_4$	2.494325	9.943	17	−1.4	17
47	$6d[7/2]_4$	3.506969	11.023	107	−31	107
48	$7d[7/2]_4$	4.512464	11.461	340	−3800	340
49	$6s'[1/2]_0$	1.846778	9.445	–	0.6	11
50	$7s'[1/2]_0$	2.945265	11.865	–	14	72
51	$8s'[1/2]_0$	3.945265	12.559	–	79	230
52	$6s'[1/2]_1$	1.875812	9.568	23	0.6	11
53	$7s'[1/2]_1$	2.954575	11.875	110	19	72
54	$8s'[1/2]_1$	3.974836	12.572	350	80	240
55	$6p'[1/2]_0$	2.434749	11.139	–	2.6	29
56	$7p'[1/2]_0$	3.434749	12.28	–	33	125
57	$8p'[1/2]_0$	4.434749	12.741	–	210	360
58	$6p'[1/2]_1$	2.397397	11.067	–	2.7	24
59	$7p'[1/2]_1$	3.397397	12.255	–	44	110
60	$8p'[1/2]_1$	4.397397	12.73	–	280	330
61	$6p'[3/2]_1$	2.342837	10.955	–	3.3	24
62	$7p'[3/2]_1$	3.342837	12.216	–	34	110

Table 1 (continued)

#	Level	n^*	E, eV	$\bar{C}_3$	$\bar{C}_4$	$\bar{C}_6$
63	$8p'[3/2]_1$	4.342837	12.712	–	230	330
64	$6p'[3/2]_2$	2.390129	11.052	–	2.8	26
65	$7p'[3/2]_2$	3.390129	12.25	–	260	120
66	$8p'[3/2]_2$	4.390129	12.727	–	260	340
67	$5d'[3/2]_1$	2.727304	11.605	–	−4.1	29
68	$6d'[3/2]_1$	3.714424	12.449	–	−0.1	140
69	$7d'[3/2]_1$	4.707171	12.821	–	130	405
70	$5d'[3/2]_2$	2.546386	11.337	–	−11	20
71	$6d'[3/2]_2$	3.546386	12.354	–	−8	110
72	$7d'[3/2]_2$	4.546386	12.777	–	−70	350
73	$5d'[5/2]_2$	2.524493	11.3	–	−0.8	19
74	$6d'[5/2]_2$	3.524493	12.34	–	−21	110
75	$7d'[5/2]_2$	4.524493	12.771	–	−160	340
76	$5d'[5/2]_3$	2.569191	11.374	–	−0.1	21
77	$6d'[5/2]_3$	3.569191	12.372	–	−3.6	115
78	$7d'[5/2]_3$	4.569191	12.784	–	−43	360

The technique of measurement of the electron concentration N_e from the width of a spectral line of inert gases does not loss its urgency within the framework of the model of meta-equilibrium plasma. (Remind that the value of N_e obtained in such a way may fail meeting the Saha–Boltzmann equations.) For $N_e \geq 10^{16}$ cm^{-3} the line width is proportional to the electron concentration. At $N_e < 10^{16}$ cm^{-3} the contribution of the van der Waals collisional broadening is significant. Its value is proportional to the concentration of atoms. To determine the electron concentration, we should subtract the van der Waals component γ_6 proportional to the concentration of atoms from the width of the line under study (18).

Table 3 gives the line widths of the Xe atom caused by different broadening mechanism and related to one atom (electron): γ_{4e}/n_e, $\gamma_{\langle\sigma v\rangle}/n_e$, γ_6/n_a, and γ_3/n_a for the temperature T_e = 0.5, 0.7, and 0.9 eV. These values correspond to the slope of a straight line on the plot of the line width dependence on the electron concentration $\gamma = \gamma(N_e)$. Given the experimental width, we can determine the electron concentration ($\gamma = \frac{1.24 \cdot 10^4}{\lambda^2}\Delta\lambda$, where γ is expressed in eV, and λ and $\Delta\lambda$ are given in Å).

Table 2. Experimental values of the shift δ, width γ, ratio γ/δ from Ref. 10 and our calculation by Eq. (18), in 10^{-7} eV; $N_e \sim 6 \cdot 10^{13}$ cm^{-3}

Transition	λ, nm	δ_{exp}	γ_{exp}	$\gamma_{exp}/\delta_{exp}$	γ (18)
$6s[3/2]_1 \to 6p[1/2]_0$	827.99	−2.5(0.5)*	5(0.6)	20	4.8
$6s[3/2]_1 \to 6p[3/2]_2$	895.2	1.2(0.2)	5.(0.1)	4.2	4.5
$6s[3/2]_1 \to 6p[3/2]_1$	916.24	0.6(0.2)	–	–	4.8
$6s[3/2]_2 \to 6p[3/2]_2$	823.1	0.(0.3)	≤ 2.5(2.0)	–	2.8
$6s[3/2]_2 \to 6p[3/2]_1$	840.89	0.5(0.2)	1.24(0.7)	2.5	3.4
$6s[3/2]_2 \to 6p[3/2]_3$	881.91	0.12(0.5)	≤ 2.5(2.0)	21.0	2.5
$6s[3/2]_2 \to 6p[5/2]_2$	904.51	0.37(0.2)	1.25(0.8)	3.4	2.4
$6s[3/2]_1 \to 7p[1/2]_0$	480.69	1.(0.3)	5.(2.0)	5.0	7.8
$6s[3/2]_1 \to 7p[3/2]_1$	482.96	1.(1.)	7.5(2.0)	7.5	9.3
$6s[3/2]_1 \to 7p[3/2]_2$	484.32	2.5(0.2)	7.5(3.0)	3.0	17.0
$6s[3/2]_1 \to 7p[5/2]_2$	492.3	1.6(0.4)	7.5(2.0)	4.7	9.5
$6s[3/2]_2 \to 7p[3/2]_2$	462.41	2.4(0.3)	7.5(1.5)	3.1	15.0
$6s[3/2]_2 \to 7p[5/2]_3$	467.11	2.(0.4)	7.5(2.0)	3.8	7.4
$6s[3/2]_2 \to 7p[5/2]_2$	469.69	2.1(0.25)	5.(2.0)	2.4	8.1
$6s[1/2]_1 \to 6p[1/2]_1$	826.6	1.(0.1)	3.7(0.5)	3.7	3.2
$6s[1/2]_1 \to 6p[3/2]_2$	834.66	0.5(0.2)	3.7(1.0)	7.4	3.3
$6p[1/2]_1 \to 6d[3/2]_2$	873.91	0.25(0.1)	5.(0.6)	20.0	48.0
$6p[1/2]_1 \to 6d[1/2]_0$	890.84	1.24(0.5)	3.7(0.6)	3.0	7.4
$6p[1/2]_1 \to 7d[3/2]_2$	646.95	1.5(0.2)	7.5(0.7)	5.0	40.0
$6p[1/2]_1 \to 7d[3/2]_1$	647.26	1.5(0.6)	6.2(4.0)	4.1	40.0
$6p[3/2]_1 \to 7d[5/2]_2$	728.51	1.6(0.3)	7.5(0.7)	4.7	40.0

* The minus sign means the blue shift; the value in parenthesis is the relative measurement error.

Table 3. Values of γ_{4e}/n_e, $\gamma_{\sigma v}/n_e$, γ_6/n_a, and γ_3/n_a for the temperature T_e = 0.5, 0.7, and 0.9 eV

Transition λ, Å	T_e, eV	γ_{4e}/n_e, eV/cm^{-3}	$\gamma_{<\sigma v>}/n_e$, eV/cm^{-3}	γ_6/n_a, eV/cm^{-3}	γ_3/n_a, eV/cm^{-3}
$6s[3/2]_1 \to 6p[1/2]_0$ 8279.9	0.5	0.0074	0.0108	5.69E−06	3.96E−6
	0.7	0.008	0.0104	6.1 E−06	4.0 E−6
	0.9	0.0082	0.0092	6.75E−06	4.19E−6
$6s[3/2]_1 \to 7p[1/2]_0$ 4806.9	0.5	0.0111	0.0286	1.06E−05	3.96E−6
	0.7	0.0121	0.0282	1.19E−05	4.0 E−6
	0.9	0.0126	0.028	1.29E−05	4.19E−6
$6s[3/2]_{1,2} \to 7p[1/2]_1$ 5028.1; 4792.5	0.5	0.0156	0.0187	1.03E−05	3.96E−6
	0.7	0.0168	0.0177	1.13E−05	4.0 E−6
	0.9	0.0173	0.0166	1.28E−05	4.19E−6
$6s[3/2]_{1,2} \to 7p[3/2]_1$ 4829.6; 4611.8	0.5	0.0188	0.0412	1.07E−05	3.96E−6
	0.7	0.0196	0.0313	1.29E−05	4.0 E−6
	0.9	0.0204	0.026	1.28E−05	4.19E−6
$6s[3/2]_{1,2} \to 7p[3/2]_2$ 4843.2; 4624.1	0.5	0.0926	0.0861	1.07E−05	3.96E−6
	0.7	0.0966	0.0929	1.19E−05	4.0 E−6
	0.9	0.1019	0.1066	1.29E−05	4.19E−6
$6s[3/2]_{1,2} \to 7p[5/2]_2$ 4923.0; 4696.9	0.5	0.0231	0.0477	1.06E−05	3.96E−6
	0.7	0.0257	0.0446	1.18E−05	4.0 E−6
	0.9	0.0257	0.0456	1.28E−05	4.19E−6
$6s[3/2]_2 \to 7p[5/2]_3$ 4671.1	0.5	0.0257	0.0258	1.05E−05	0
	0.7	0.0276	0.0270	1.16E−05	0
	0.9	0.0278	0.0208	1.25E−05	0

N o t e . 5.69E−06 means $5.96 \cdot 10^{-6}$ and so on.

Spectral line profile of cylindrical plasma column with variable electron concentration

In Ref. 7, the "method of localizations" was proposed, which allows the local emissivity of plasma of inhomogeneous objects possessing the axial symmetry to be determined without using traditional inversion methods. This method was based on the fact that the plasma emissivity decreases fast with temperature drop at a constant pressure, and, as a consequence, the total emission, measured experimentally, is mostly caused by the axial zones of a plasma body.

Reference 7 considers an inhomogeneous plasma body, the pressure in which is constant and the temperature distribution along the observation line is symmetric and has the parabolic shape.

In numerical simulation, the formal solution of the transfer equation

$$I_\lambda(\tau) = I_\lambda(0)\exp(-\tau) + \int_0^\tau I_{\lambda P}(\tau')\exp(\tau' - \tau)\mathrm{d}\tau';$$

$$\tau = \int_y^\infty x_\lambda(y')\mathrm{d}y' \qquad (19)$$

is used to determine the radiation intensity. A numerical algorithm reduces the solution to the recurrent equation relating the radiation intensity at neighboring points:

$$I_\lambda(\tau_i) = I_\lambda(\tau_{i-1})\exp(-\Delta\tau_i) + I_{\lambda P}(\tau_i)\times$$
$$\times[1-\exp(-\Delta\tau_i)] - \left(\frac{\mathrm{d}I_{\lambda P}}{\mathrm{d}\tau}\right)_i [1-\exp(-\Delta\tau_i)(1+\Delta\tau_i)]. \qquad (20)$$

The spectral absorption coefficient x_λ has the form

$$x_\lambda = \pi e^2 f_{nm} N_\mathrm{e}\varphi(\lambda)/(mc). \qquad (21)$$

Since the central part of the profile is caused by collisions with electrons, the profile is a Lorentzian one with the halfwidth $\gamma/2$ and the shift δ proportional to the electron concentration and weakly dependent on the temperature.

In the non-traditional part of the diagram of meta-equilibrium states of the inert gas plasma, we have another situation: the electron temperature varies insignificantly, and the electron concentration, for example, over the radius of the cylindrical column may decrease by an order of magnitude.

Let us specify the decrease of the electron concentration over the radius (r = 1 cm) as is shown in Fig. 1 (curve *1*) or assume that it is constant (curve *2*). Then consider the profile of the line corresponding to the transition $6s[3/2]_1 \to 7p[1/2]_0$ in absorption at $\lambda = 4810.9$ Å XeI. The line width is caused, as in the above case, by the square Stark effect, and the constant is $C_4 = -27\cdot10^{-14}$ cm$^4\cdot$s^{-1} (blue shift). The calculations are carried out formally by Eqs. (19)–(21) in the very simplified version for four cases:

1) N_e is specified according to curve *1* (see Fig. 1) and the lower level population and temperature are determined from solution of equations of the sublevel kinetics for the xenon plasma[8] at the given number of nuclei (diagrams of meta-equilibrium states of Xe);

2) N_e is specified according to curve *1* and the lower level population and temperature are calculated using the Saha–Boltzmann equations at known N_e and the density;

3) N_e = const, the lower level population and the temperature are determined from solution of the equations of sublevel kinetics;

4) N_e = const, the lower level population and the temperature are calculated using the Saha–Boltzmann equations at known N_e and the density.

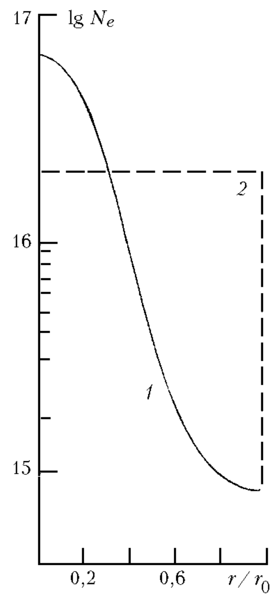

Fig. 1. Distribution of electron concentration over the radius.

Figure 2 shows the profile of the line at $\lambda = 4810.9$ Å XeI for the cases listed above. The first two cases are shown in Fig. 2*a*, the third case for $N_\mathrm{e} = 2\cdot10^{16}$ cm^{-3} corresponds to curve *1* in Fig. 2*b*, and the fourth case corresponds to curve *2*.

Curve *2* in Fig. 2*a* is obtained in the same way as the profiles in Ref. 7 and is asymmetric as well. Curve *1* in this figure has an unusual shape. The similar shape was observed in Ref. 9, which presented a microphotogram (shown in Fig. 2*c*) for the argon plasma in the spark discharge (curve *1*). This shape is compared with curve *2* corresponding to the spectrum of hollow cathode plasma (plasma parameters differ insignificantly). The left line in the microphotogram *2* coincides with the peak of curve *1* (Fig. 2*c*), i.e., the transition wavelength is the same in the first and the second cases. However, the left peak is complemented with a second "wide line." Actually, the peak and the "wide line" form the profile of one transition, whose behavior is similar to curve *1* in Fig. 2*a* (shifts are different because of the sign of the constant C_4).

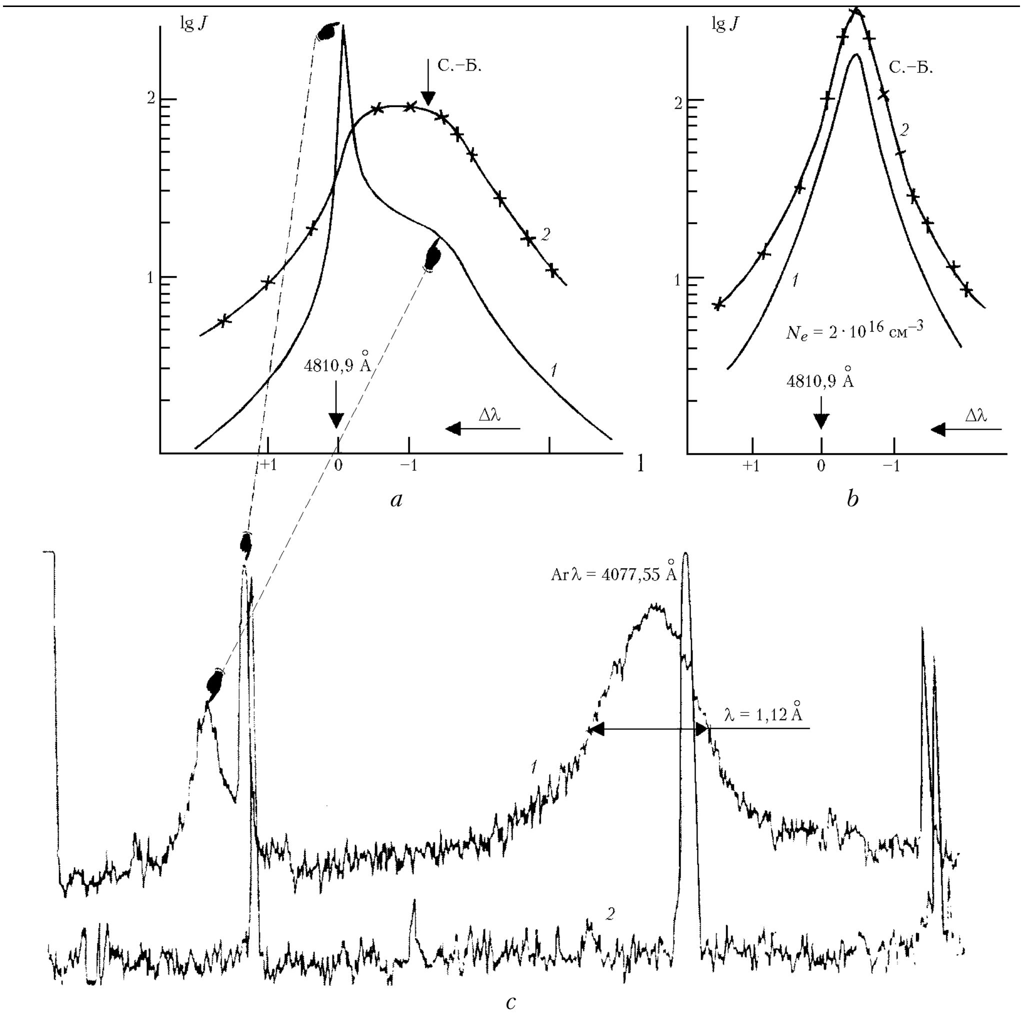

Fig. 2. Calculated intensity of XeI line at λ = 4077.55 Å (*a*, *b*) (Saha–Boltzmann), microphotogram of ArII lines,[9] arrows show the identity in the profile behavior (*c*).

Conclusion

As a result of numerical solution of the system of equations of sublevel kinetics, we have obtained the diagrams of meta-equilibrium states of inert gas plasma that establish one-to-one correspondence between the electron concentration, gas density, and the given electron temperature. The meta-equilibrium states are characterized by the distributions of the excited states different from the Boltzmann distribution and having the shape of a polyline.

The characteristics of line profiles in absorption spectra of the inhomogeneous low-temperature plasma have been studied in the case that the electron concentration decreases over the radius by an order of magnitude and even more. The mechanisms of broadening of spectral lines have been studied for the meta-equilibrium plasma. The tabulated data are presented that allow estimating for the case of the meta-equilibrium plasma. Recommendations for diagnostics of plasma are given.

References

1. H.R. Griem, *Spectral Line Broadening by Plasmas* (Academic Press, New York, 1974).
2. E.P. Skorokhod, A.Yu. Gavrilova, A.G. Kiselev, et al., Atmos. Oceanic Opt. **13**, No. 3, 252–255 (2000).
3. A.Yu. Gavrilova, A.G. Kiselev, E.P. Skorokhod, and O.F. Reshetnikov, Mat. Modelir. **11**, No. 6, 31–35 (1999).
4. I.I. Sobelman, *Introduction to Theory of Atomic Spectra* (Fizmatgiz, Moscow, 1963), 463 pp.
5. E.P. Skorokhod and Yu.K. Zemtsov, *Broadening of Spectral Lines of Xenon Plasma* (VINITI, Moscow, 1981), No. 3574–81, 65 pp.
6. Yu.K. Zemtsov and E.P. Skorokhod, *Broadening Constants for Spectral Lines of Xenon Atom* (VINITI, Moscow, 1981), No. 3575–81, 40 pp.
7. E.A. Ershov-Pavlov and K.L. Stepanov, "*Formation of line spectrum in emission of inhomogeneous plasma volumes*," Preprint No. 8, Institute of Molecular and Atomic Physics, Minsk (2000), 18 pp.
8. A.G. Kiselev and E.P. Skorokhod, in: *Burning and Electrodynamic Phenomena* (Publishing House of Chuvashskii State University, Cheboksary, 1999), pp. 104–110.
9. M.A. Mazing, "*Broadening and shifting of spectral lines in gas-discharge plasma*," Cand. Phys. Math. Sci. Dissert., Moscow (1959).
10. D.A. Jack Son, J. Opt. Soc. Am. **66**, 1014–1016 (1976).